Regional Dysfunction After Myocardial Infarction in Rats

Emil K.S. Espe, MSc, PhD*; Jan Magnus Aronsen, MD*; Morten Eriksen, MD, PhD; Ole M. Sejersted, MD, PhD; Lili Zhang, MSc, PhD; Ivar Sjaastad, MD, PhD

Background—Detailed understanding of regional function after myocardial infarction (MI) is currently incomplete. We aimed at investigating regional myocardial strain and work in post-MI rats with and without heart failure.

Methods and Results—Six weeks after induction of MI, 62 male Wistar-Hannover rats with a range of infarct sizes, plus 14 sham-operated rats, were examined by cine and phase-contrast magnetic resonance imaging. After magnetic resonance imaging, the rats were catheterized, and left ventricular pressures were recorded. Regional strain and work were calculated from the magnetic resonance imaging and pressure data. On the basis of end-diastolic left ventricular pressure, 34 MI rats were classified as nonfailing (MI_{NF}) and 28 MI rats as failing (MI_{CHF}). In the region remote to the infarct, the MI_{NF} rats exhibited preserved strain and increased work compared with sham, whereas MI_{CHF} had reduced longitudinal strain and no increase in work in this region. In the noninfarcted region adjacent to the infarct, MI_{CHF} demonstrated substantially reduced work because of high levels of negative work.

Conclusions—We have demonstrated a distinct difference in regional work between nonfailing and failing hearts after MI and offer novel insight into the relation between regional function and presence of congestion. Work analysis provided significant added value over strain analysis alone. (***Circ Cardiovasc Imaging*. 2017;10:e005997. DOI: 10.1161/CIRCIMAGING.116.005997.**)

Key Words: heart failure ■ infarction ■ magnetic resonance imaging ■ myocardial infarction ■ rats

After myocardial infarction (MI), the surviving myocardium undergoes a complex cascade of changes as a part of the cardiac adaptation to the sudden loss of viable myocardium. Lack of successful compensation may ultimately lead to congestive heart failure.

See Editorial by Rademakers
See Clinical Perspective

Cardiac function subsequent to MI might vary considerably even if the scar size is similar,[1] and the workload varies regionally across the noninfarcted myocardium.[2] Detailed understanding of the regional mechanical response to MI with variable sizes is currently incomplete. Particularly, the functional implications in regions remote to the infarct remain unclear; studies have reported both preserved[3–5] and reduced[6–8] strain after MI in remote regions. Several issues might be responsible for this apparent discrepancy, including differences in disease severity, methodology, time of investigation, and dissimilarities between species.[6] Moreover, direct comparison of myocardial strain as a measure of myocardial function is challenging because it does not account for differences in loading conditions.[9,10]

The post-MI rat is a well-established model of post-MI remodeling and exhibits both nonfailing and failing phenotypes.[11] Magnetic resonance imaging (MRI) is emerging as a technique allowing robust assessment of in vivo regional myocardial function, and it has also recently been demonstrated that phase-contrast MRI (PC-MRI) allows examination of regional alterations in myocardial function in small animals with very high resolution,[12,13] including the possibility to account for loading conditions and obtain in vivo regional myocardial work.[2]

In the present study, we sought to investigate regional strain and work in post-MI rats with different degree of heart failure and aimed this way to elucidate the apparent discord in the literature on regional function after MI. We hypothesized (1) that the failing and nonfailing groups exhibit different distribution of regional strain and work, and (2) that analysis of work offers added value over strain alone.

Methods

Animal Preparation

Male Wistar-Hannover rats (≈300 g) were anesthetized (64% N_2O, 32% O_2, and 4% isoflurane) and ventilated by endotracheal intubation using a Zoovent ventilator. In 62 of the rats, left ventricular (LV) MI was induced by proximal ligation of the left coronary artery during maintained anesthesia (66% N_2O, 32% O_2, and 1.5–2.5% isoflurane). The placement of the ligation was deliberately varied to achieve variable infarct sizes. Fourteen rats underwent the same procedure except ligation to serve as sham-operated controls. All experimental

Received November 29, 2016; accepted July 7, 2017.

From the Institute for Experimental Medical Research, Oslo University Hospital and University of Oslo, Norway (E.K.S.E., J.M.A., O.M.S., L.Z., I.S.); Bjørknes College, Oslo, Norway (J.M.A.); and Respinor AS, Oslo, Norway (M.E.).

*These authors contributed equally to this work and share first authorship.

The Data Supplement is available at http://circimaging.ahajournals.org/lookup/suppl/doi:10.1161/CIRCIMAGING.116.005997/-/DC1.

Correspondence to Emil K.S. Espe, MSc, PhD, Institute for Experimental Medical Research, Oslo University Hospital, PB-4956 Nydalen, NO-0424 Oslo, Norway. E-mail ekespe@medisin.uio.no

protocols were approved by the Norwegian National Animal Research Authority and performed in accordance with the European Directive 2010/63/EU and institutional guidelines (ID 3284).

Pursuing the goal of reducing number of animals used in experimental research,[14] cine MRI data (infarct size, volumes, and ejection fraction), pressure data (peak and end-diastolic LV pressures [LVPs]), heart rate, and heart, lung, and body weight from a subset of the animals included here have also been reported previously.[15]

Magnetic Resonance Imaging

Six weeks after operation, MRI experiments were performed on a 9.4-T magnetic resonance system (Agilent Technologies, Inc) using hardware dedicated to rat cardiac imaging.[13] Anesthesia was induced in a chamber using a mixture of O_2 and 4.0% isoflurane and maintained during acquisition in freely breathing animals using O_2 and ≈1.5% isoflurane. Throughout the examination, ECG, respiration, and body temperature were monitored continuously, the latter maintained at 37.0°C by heated air. LV short-axis imaging planes were identified from untriggered scout images, and all subsequent acquisitions triggered at the peak of the R wave and gated for respiratory motion. In all data sets, the temporal resolution was equal to the repetition time.

Cine MRI

A stack of short-axis cine MRI slices covering the entire LV was acquired using an RF-spoiled gradient echo sequence. Imaging parameters were echo time=1.97 ms, repetition time=2.80 ms, field of view=45×45 mm, matrix=192×192 after 2× zero filling, slice thickness=1.5 mm, average number of slices per heart=10; flip angle 15°, signal averaging=3×, acquisition time for a complete stack ≈20 minutes.

Also, a single oblique slice showing the mitral and aortic valve was acquired, with a temporal coverage of >100% of the R-R interval. Imaging parameters were echo time=2.04 ms, repetition time=2.96 ms, field of view=50×50 mm, matrix=128×128, slice thickness=2.0 mm, flip angle=15°, signal averaging=3×, acquisition time=2 to 3 minutes.

Phase-Contrast MRI

PC-MRI used an RF-spoiled black blood gradient echo cine sequence using 9-point velocity-encoding and rotating field of view.[13,16,17] Three short-axis slices were positioned +3, 0, and −3 mm from the long-axis midpoint of the LV (labeled apical, midventricular, and basal slices; Figure 1A). All three slices were parallel and shared a common center normal. The PC-MRI time series also covered >100% of the R-R interval. Imaging parameters were echo time=2.22 to 2.26 ms, repetition time=2.93 to 3.21 ms, field of view=50×50 mm, matrix=128×128, slice thickness=1.5 mm, flip angle=7°, velocity encoding strength=13.9 cm/s, signal averaging=2× using rotating field of view,[13] total acquisition time=45 to 50 minutes.

LVP Measurements

Forty-eight hours after MRI, the rats were anesthetized (using the same setup and settings as during MRI examination) and catheterized using a micromanometer-tipped catheter (Samba Systems, Sweden) inserted retrogradely via the right common carotid artery into the LV cavity. Maximum and end-diastolic LVPs were measured, labeled LVP_{max} and LVP_{ED}, respectively. LVP_{ED} was measured immediately before the steep rise in the pressure curves caused by systolic contraction. After removing the catheter, the heart was excised in deep surgical anesthesia. The hearts and lungs were weighed in 64 rats.

The rats were stratified according to a previously established threshold based on LVP_{ED}.[11,15] In brief, these studies demonstrated that a threshold of LVP_{ED}=15 mm Hg successfully differentiated between post-MI rats with and without characteristics of congestive heart failure. Accordingly, we classified rats with LVP_{ED} ≥15 mm Hg as failing (MI_{CHF}) and rats with LVP_{ED} <15 mm Hg as nonfailing (MI_{NF}). LVP curves for all animals were generated by temporally matching the group-specific standard curves to the LV valvular events and scaling to LVP_{max} and LVP_{ED}.[10]

Standard Pressure Curve Generation

In 17 rats (sham/MI_{NF}/MI_{CHF}=5/7/5), LVP curves for the entire cardiac cycle were recorded concurrently with measurement of mitral and aortic valve flow by Doppler echocardiography using a Vevo 2100 ultrasound scanner (FUJIFILM VisualSonics Inc, Canada). This allowed determination of the timing of opening and closing of the mitral and aortic valves in relation to the LVP curve waveform. Three standard LVP curves were generated from the pressure measurements, one for each group, by normalizing to peak pressure and temporal matching to the valvular events.[10]

MRI Post-Processing

End diastolic and end systolic ventricular volumes were measured by segmenting end-systolic and end-diastolic cine MRI slices and adding the contributions of each slice. Stroke volume, cardiac output, and ejection fraction were calculated. Infarct size was measured by demarking regions of akinesia, lacking radial thickening in end systole.[18] From the valve cine loop, timing of aortic and mitral valve opening and closure relative to the R peak was determined.

Calculation of Myocardial Strain

In each PC-MRI slice, the myocardium was segmented using a semiautomatic method previously described.[19] In brief, this requires the user to delineate the endo- and epicardium at end systole and end diastole, before the masks were automatically propagated throughout the cardiac cycle based on the underlying velocity information.[19] The myocardial masks were then divided into 32 equal sectors.[16] In each MI heart, the noninfarcted myocardium was divided into 6 regions of equal size which were pairwise pooled to form the remote zone (RZ), medial zone (MZ), and adjacent zone (AZ; Figure 1B), serving as the basis for comparison of regional features. For each of the 3 slices, a set of zones were generated for the sham hearts, based on the average position of the 3 zones from the infarcted hearts. The only exception from this was when the sum of work done per zone was compared, where 2 different sets of sham zones were used to match the different sizes of the MI_{NF} and MI_{CHF} zones. This allowed comparison of the total work done per zone.

In each slice, time-resolved regional wall thickness and regional short-axis radius of curvature (ROC) were automatically calculated as previously described from the PC-MRI segmentation masks (Figure 1D).[2] The data were filtered using a running average of 3 sectors. Moreover, time-resolved regional long-axis ROC was calculated in the same fashion sectorwise using the relative position of the corresponding sectors in the 3 slices. Then, biplane average ROC was calculated as follows,[10] where ROC_S is short-axis radius of curvature and ROC_L is long-axis radius of curvature:

$$\frac{1}{ROC(t)} = \frac{1}{2}\left(\frac{1}{ROC_S(t)} + \frac{1}{ROC_L(t)}\right) \quad (1)$$

To assess variability of the curvature measurement, a second observer redid the ROC measurement in 12 animals (n=4/4/4 for sham/MI_{NF}/MI_{CHF}). Interobserver variability was evaluated in the 3 zones using Bland–Altman limits of agreement.

Three-dimensional myocardial velocity vectors were reconstructed from the PC-MRI data in each pixel.[13] Because the acquisition covered >100% of the cycle, the heart rate could be determined from the velocity waveforms. Three-dimensional pixelwise myocardial motion paths were constructed using temporal integration of the 3-dimensional velocities,[20,21] and circumferential strain was calculated in each sector.[13] This was done by calculating the average displacement of all pixels contained in each sector and using the relative displacement of the center of mass in neighboring sector pairs to calculate strain between each pair. Similarly, sectorwise longitudinal strain was calculated using the motion paths from the basal and apical slices. Finally, regional area strain (S) was calculated from circumferential and longitudinal strain as follows,[10] where S_C is circumferential strain and S_L is longitudinal strain:

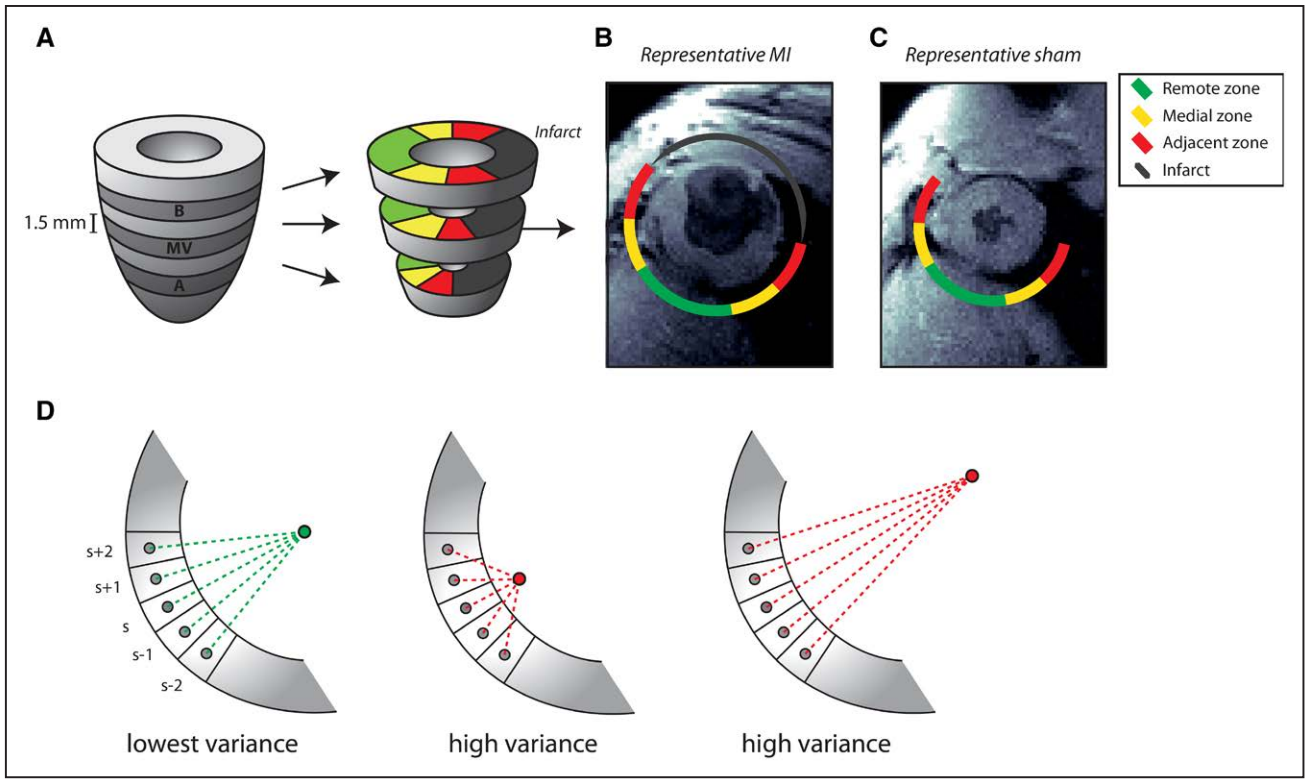

Figure 1. Geometry. **A**, The positioning of the basal, midventricular, and apical phase-contrast magnetic resonance imaging (PC-MRI) slices in the left ventricle. **B**, **C**, Definition of the 3 noninfarcted zones in a midventricular representative myocardial infarction (MI) slice (**B**) and the correspondingly localized regions in a representative sham (**C**). The zones, shown here is end systole, followed the myocardium throughout the cardiac cycle by exploiting the underlying velocity data. **D**, Calculation of radius of curvature (ROC) for a sector *s* in a given slice. The green point is identified, at which the variance in distance (dashed lines) to the center of 5 sectors surrounding *s* is at its minimum. Then, the ROC in sector *s* is found as the average length of the 5 green dashed lines. The process is repeated for all 32 sectors. The red points are 2 random examples of higher variance.

$$S(t) = \left(1 + S_C(t)\right)\left(1 + S_L(t)\right) - 1 \quad (2)$$

Moreover, the correlation between the regional and global S waveforms served as a measure of regional coherence.[22] All post-processing was done with the operator blinded to animal group.

Calculation of Myocardial Work and Stress

Regional myocardial work was calculated as previously described.[2,10] In brief, this involved multiplication of LVP, ROC, and the temporal derivative of S to get instantaneous myocardial power per unit surface area, whose temporal integral yielded work per unit surface area (note that in this context, area refers to the inner wall of the myocardium, ie, not cross-sectional area). Work per unit long-axis length was found by multiplying work per unit surface area with the circumferential length of the sector, and work per mass was found by dividing work per unit surface area by regional wall thickness and using a conversion factor of 1.05 g/cm^3.

The concept of wasted work quantifies to what degree positive work is lost because of stretching of the myocardium in systole.[23] Systolic negative work per unit length was found by integrating only positive-valued strain rates (ie, stretching) from mitral valve closure to aortic valve closure. Wasted work was found as the ratio of the total negative and positive work over the entire viable myocardium.[23]

Regional wall stress was estimated by multiplying LVP and regional ROC and dividing by regional wall thickness. For comparison of regional parameters in each of the 3 zones, data from the individual zones in all slices were pooled and averaged weighted by the estimated wall volume (estimated as circumferential length multiplied by wall thickness).

To assess the impact of the usage of group-specific standard pressure curves, we performed a supplementary calculation using a group-unspecific standard pressure curve. The details are given in the Data Supplement.

Statistics

All analysis was done using Matlab (The MathWorks) applying the 2-sided Mann–Whitney *U* test or Kruskall–Wallis nonparametric test with Dunn–Sidak post hoc test. The Spearman rank correlation coefficient was used in the calculation of regional coherence.[22] Interobserver variability was evaluated using Bland–Altman limits of agreement. Statistical significance was inferred for $P < 0.05$. All parameters are reported with mean and SE.

Results

Animal Data and Global MRI Parameters

Twenty-eight MI rats had $LVP_{ED} \geq 15$ mm Hg and were placed in the MI_{CHF} group, whereas the remaining 34 MI rats were placed in the MI_{NF} group (Table 1). As expected, the MI_{CHF} hearts exhibited increased heart and lung weight compared with sham and MI_{NF}.

The mean infarct was 73% larger in the MI_{CHF} group than in the MI_{NF} group (Table 2), but with substantial overlap (range MI_{NF}: 1.6%–39.0%, MI_{CHF}: 27.3%–51.5%). Compared with sham, the MI_{NF} hearts had increased LV volumes and reduced ejection fraction, but preserved cardiac output. The MI_{CHF} hearts had higher ventricular volumes compared with

Table 1. Animal Data

Parameter	Sham (n=14)	MI_{NF} (n=34)	MI_{CHF} (n=28)
LVP_{max}, mm Hg	124 (4)	122 (3)	105 (2)*†
LVP_{ED}, mm Hg	2.1 (0.3)	5.9 (0.5)*	26.1 (0.8)*†
Parameter	Sham (n=14)	MI_{NF} (n=23)	MI_{CHF} (n=27)
Body weight, g	408 (6)	415 (9)	418 (14)
Heart weight, g	1.27 (0.06)	1.56 (0.09)	2.29 (0.10)*†
Lung weight, g	1.38 (0.07)	1.68 (0.07)	4.18 (0.19)*†

Data are mean (SEM). LVP_{ED} indicates end-diastolic left ventricular pressure; LVP_{max}, peak left ventricular pressure; MI_{NF}, myocardial infarction without heart failure; MI_{CHF}, myocardial infarction with heart failure.

*P<0.05 compared with sham.

†P<0.05 compared with MI_{NF}.

both sham and MI_{NF}, as well as reduced heart rate and ejection fraction. Cardiac output was lower in MI_{CHF} than in MI_{NF}.

Distribution of Regional Myocardial Strain

Strain curves from representative animals are found in Figure 2. Peak strain varied regionally in all groups, including sham (Figure 3). Remote to the infarct, MI_{NF} exhibited preserved strain compared with sham, whereas longitudinal and area strains were reduced in the MI_{CHF} group compared with both sham and MI_{NF}. Adjacent to the infarct, all strain components were reduced in both MI groups compared with sham. Lower area strain coherence signified lack of uniform contraction in both MI groups, more pronounced in MI_{CHF} than in MI_{NF}, which worsened toward the infarct.

Regional Redistribution of Myocardial Work and Stress

To investigate the association between regional strain and myocardial work in post-MI rats, we next calculated regional work, including negative work, in the same regions as the strain calculations. Wall stress–strain loops from representative animals, whose area represent work per unit volume, are shown in Figure 2. The results from the work analysis are shown in Figure 4. Interobserver limits of agreement of ROC between the 2 observers were –0.2±1.3 mm (RZ), –0.2±1.5 mm (MZ), and –0.2±1.0 mm (AZ). Across these 12 animals, mean ROCs were 7.3 mm (RZ), 7.5 mm (MZ), and 7.1 mm (AZ).

Table 2. Global Magnetic Resonance Imaging Parameters

Parameter	Sham (n=14)	MI_{NF} (n=34)	MI_{CHF} (n=28)
Infarct size (%)		22.6 (2.0)*	39.2 (1.3)*†
Heart rate, bpm	428 (8)	431 (6)	385 (7)*†
End-diastolic volume, mL	0.33 (0.01)	0.59 (0.03)*	0.85 (0.03)*†
End-systolic volume, mL	0.09 (0.01)	0.34 (0.03)*	0.61 (0.02)*†
Stroke volume, mL	0.24 (0.01)	0.25 (0.01)	0.23 (0.01)
Ejection fraction	0.73 (0.02)	0.46 (0.03)*	0.28 (0.01)*†
Cardiac output, mL/min	103.0 (2.9)	107.9 (4.4)	90.5 (4.1)†
Wasted work ratio (%)	3.17 (0.65)	4.63 (0.65)	10.52 (1.28)*†

Data are mean (SEM). MI_{NF}, myocardial infarction without heart failure; MI_{CHF}, myocardial infarction with heart failure.

*P<0.05 vs sham.

†P<0.05 vs MI_{NF}.

Notably, the MI_{NF} hearts exhibited ≈20% increased myocardial work in the RZ compared with sham (Figure 4B). In contrast, the MI_{CHF} rats did not exhibit significantly increased myocardial work in the RZ, but rather at a comparable level as the shams (Figure 4C). In MZ and AZ, work was reduced in the MI_{CHF} hearts compared with sham. The level of negative work was correspondingly increased in the MZ and the AZ. In RZ, work per mass was not significantly different between sham and MI_{NF}, but reduced in MI_{CHF} (Figure 4F).

Compared with the sham and MI_{NF} groups, the wasted work was increased in the MI_{CHF} hearts by 230% and 130%, respectively (Table 2), signifying pronounced regional positive strain rate (ie, myocardial stretching) in systole.

Peak wall stress was not significantly different between the groups in the RZ and MZ; however, it was increased in both MI groups in the AZ (Figure 4G). Interobserver limits of agreement of ROC between the 2 observers were –0.2±1.3 mm (RZ), –0.2±1.5 mm (MZ), and –0.2 1.0 mm (AZ). Across these 12 animals, mean ROCs were 7.3 mm (RZ), 7.5 mm (MZ), and 7.1 mm (AZ).

Discussion

In the present study, we investigated in vivo regional function in the noninfarcted myocardium in 2 groups of post-MI rat hearts, nonfailing and failing. Assessment of post-MI regional function has been dominated by the analysis of deformation/strain.[3–8] In the present study, we provide a detailed analysis of regional myocardial work, which accounts for differences in loading conditions, and does therefore provide a more accurate representation of myocardial function than strain alone.[9,10]

We found that nonfailing MI hearts exhibited increased external work in the regions remote to the infarct compared with sham. In contrast, failing MI hearts demonstrated no such increase in work. Moreover, MI_{CHF} exhibited a substantial reduction in external work in the region adjacent to the infarct compared with sham. This was primarily because of a considerable increase in regional negative work because of systolic stretching, which consumes positive work done by contracting regions.

Regional Strain

Our finding of reduced strain adjacent to the infarct is in line with previous studies.[6–8] Remote to the infarct, previous studies have reported both preserved[3–5] and reduced[6–8] strain in post-MI hearts. Many factors might be responsible for this difference, including differences between methodologies, time of investigation, differences between species, and different loading conditions.[6] We found that RZ strain was preserved in nonfailing hearts but reduced in failing hearts, underlining the importance of assessing the degree of heart failure when interpreting regional function in future studies. Our findings also indicate that longitudinal strain is a more sensitive parameter for evaluating disruption of regional function, in line with previous findings.[5]

The average wall thickness was slightly higher in the AZ zone in the sham hearts (Figure 2), reducing wall stress and work per mass.

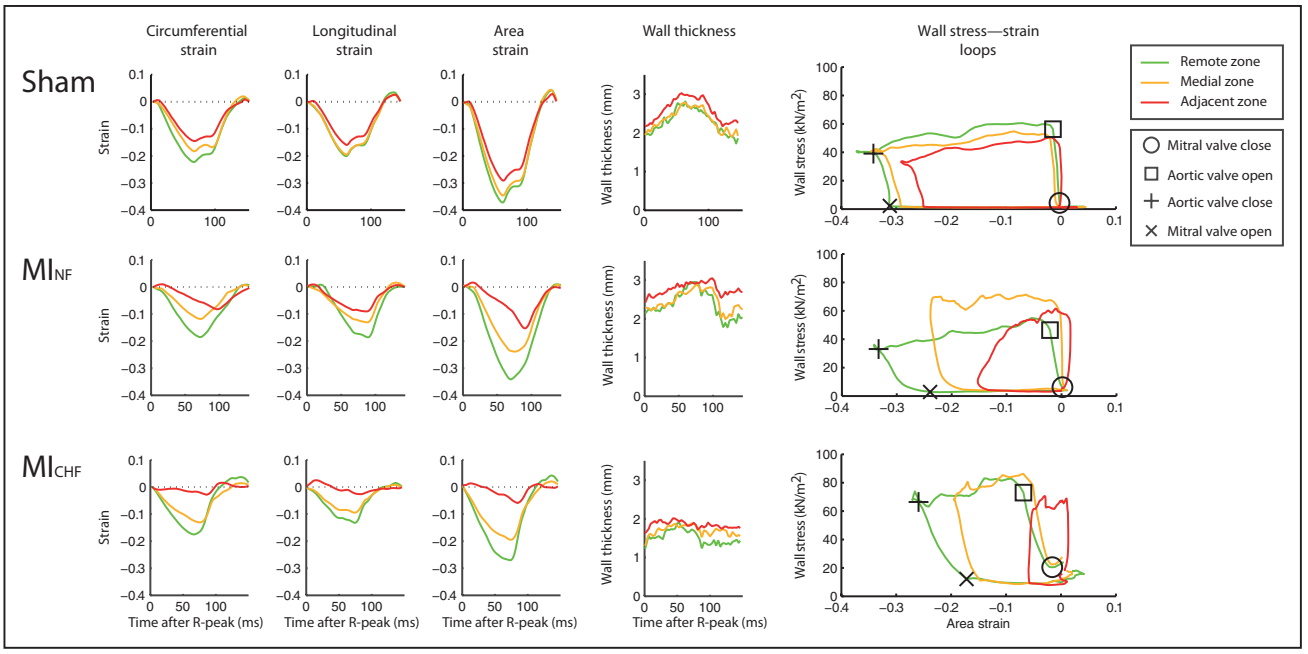

Figure 2. Representative animals. Time-resolved circumferential, longitudinal, and area strain and wall thickness for 3 representative animals, one from each group. The areas of the wall stress–strain loops represent work done per unit volume. The symbols represent valvular events (here shown only for the remote zone).

Regional Work and Stress

An infarction causes a loss of viable myocardium which, without sufficient compensation, will inevitably result in a reduced global pumping capacity. The function in the noninfarcted region of the myocardium is therefore critical. The existing literature reporting assessment of regional myocardial function is dominated by the analysis of deformation, which is load dependent.[9] Regional myocardial work accounts for loading and is therefore a more suitable measure of myocardial function than strain alone.[10] We found that the remote myocardium in the MI_{NF} hearts did more work than equivalent regions in sham. This hyperfunction was not seen by strain analysis alone, illustrating the importance of accounting for load when investigating regional function. This is in agreement with our previously published results showing increased septal work in nonfailing post-MI hearts.[2] In the current study, we show that MI_{CHF} in contrast did not exhibit any significant increase in RZ work.

In the zones closer to the infarct, regional work was substantially reduced in the MI_{CHF} hearts. For the first time, we applied the concept of wasted work[23] in post-MI hearts. The increase in negative work in MZ and AZ and higher wasted work ratio in MI_{CHF} hearts signify stretching of the myocardium during systole, also attested to by the reduction in strain coherence (Figure 3C). Consequently, a part of the positive work was wasted rather than being spent ejecting blood.[23]

High wall stress is linked to disruption of T-tubule structure and calcium homeostasis.[24] In the AZ of the infarct animals where we observed contractile dysfunction, we found that systolic stress was elevated (Figure 4G).

For a subset of the animals in the present study, we have previously reported results from myocardial quantitative polymerase chain reaction measurements.[15] In that article, we found that both the nonfailing and failing animals exhibited increased level of molecular markers of myocardial remodeling and that the animals with heart failure had higher expression of collagen type I than nonfailing in the viable LV myocardium.[15]

Limitations

We only studied the hearts 6 weeks after induction of MI and provide only a snapshot of disease progression at that point. Our findings underline the need for further investigation on post-MI alterations in myocardial function and remodeling, both with respect to regional heterogeneity, temporal dynamics, and the connection to degree of cardiac dysfunction. Particularly, to elucidate the regional mechanical adaptation to MI and its link to global function, further longitudinal studies on post-MI remodeling are necessary.

It is valuable to consider whether our observations are a result of variable intrinsic cardiac function or variable interaction with the peripheral circulation. When comparing myocardial work between the groups, we account for differences in pressure (including shape and peak of the pressure curves), which likely is the most prominent external factor affecting myocardial function. However, our data do not allow us to further elucidate the impact of other peripheral factors on regional myocardial function. Further studies are warranted to investigate the relative contribution of intrinsic and external factors on the observed dysfunction.

Our dichotomous approach does not allow us to capture the likely heterogeneity in regional function within the 2 groups.

It is worth noting that we measured regional contractile work only, hence we do not provide a direct measure of neither global nor regional myocardium metabolism. Isometric contraction and negative work also consume oxygen and likely

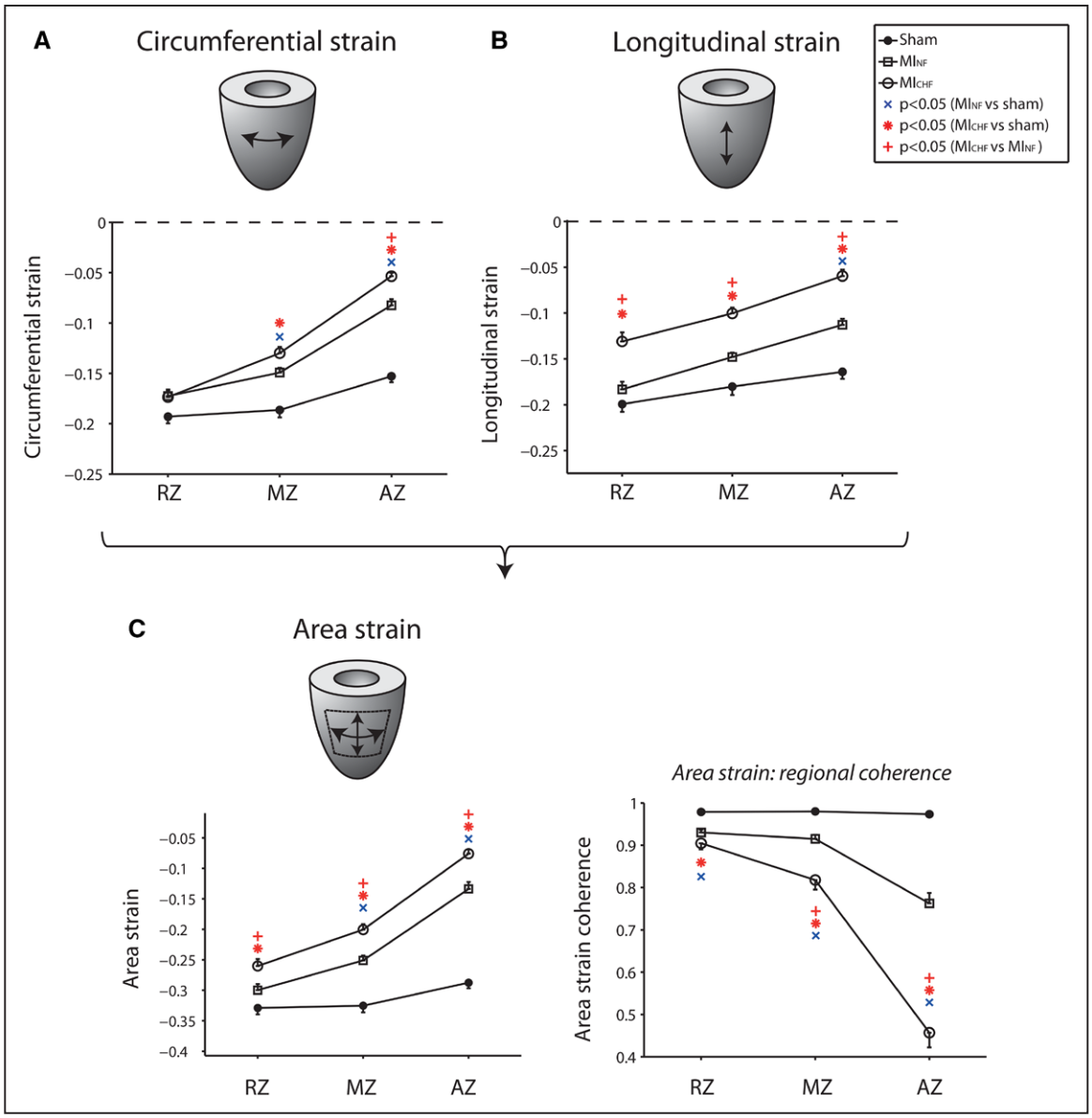

Figure 3. Regional strain. Peak myocardial circumferential (**A**), longitudinal (**B**), and area (**C**) strain. In remote zone (RZ), longitudinal and area strain were reduced in the failing (MI_{CHF}) hearts. In adjacent zone (AZ), all strain components were reduced in both myocardial infarction (MI) groups, and more so in MI_{CHF} than in nonfailing (MI_{NF}). Area strain exhibited substantial loss of coherence in AZ in MI_{CHF} hearts (**C**). (Values reported are mean with SE.) MZ indicates medial zone.

cause the energy usage to be significantly higher in MI_{CHF} than reflected by our calculations of work.

We did not perform contrast-enhanced assessment of infarct size, but relied on identification of akinesia and wall thinning. This is the recommended approach for mice with permanent coronary artery ligation, in which long-term hibernation does not occur,[18] and exhibits excellent correlation to histology-measured infarct size in rats (r=0.97).[25] Like mice, rats also lack well-established collateral circulation.[26] Figure 1B shows an end-systolic image of an infarcted heart and illustrates the discernibility of the infarct.

Conclusions

We have investigated regional myocardial function in the post-MI rat heart with and without heart failure. Rats without congestion exhibited increased work in the noninfarcted myocardium, whereas heart failure was characterized by 2 different regional features: (1) lack of increased function in regions remote to the infarct, and (2) substantial loss of external work in regions adjacent to the infarct. Work analysis provided significant added value over strain analysis alone. Our findings elucidate the association between regional function and the degree of global cardiac dysfunction, as well the importance of accounting for load when investigating regional function.

Sources of Funding

This work was supported by Center for Heart Failure Research (University of Oslo), South-Eastern Norway Regional Health Authority, Anders Jahre's Fund for the Promotion of Science, The Research Council of Norway, and Olav Raagholt og Gerd Meidel Raagholts Stiftelse for Forskning.

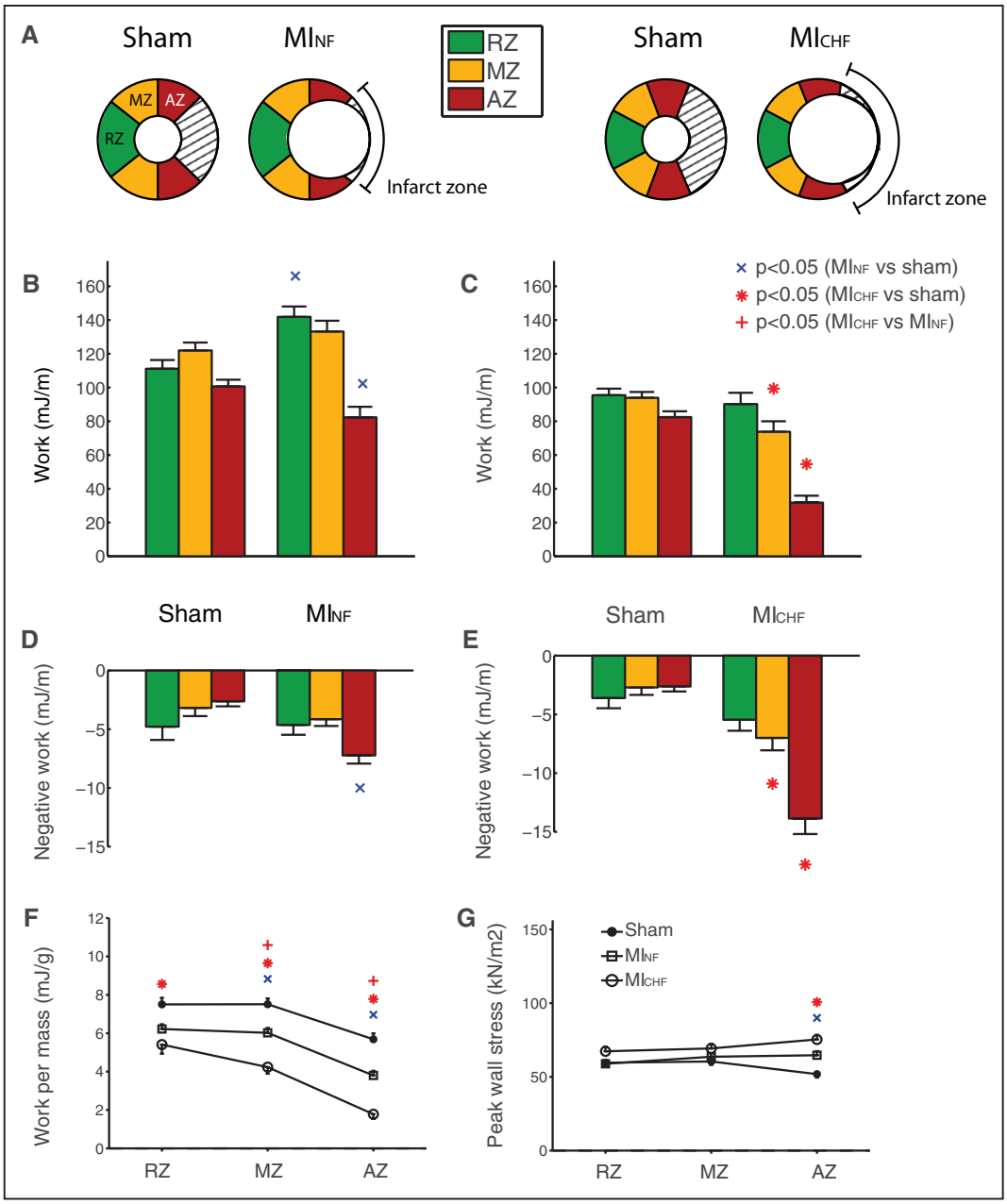

Figure 4. Regional work. The total work done in the different regions was compared between the myocardial infarction (MI) groups and equivalently sized regions in the sham (**A**). Regional work done in remote zone (RZ) was increased in the nonfailing hearts compared with equivalently sized regions in the sham hearts (**B**), and negative work in adjacent zone (AZ) was slightly higher (**D**). In the failing hearts, the work was decreased in medial zone (MZ) and AZ (**C**) and negative work was higher in both MZ and AZ (**E**). In RZ, work per mass was not significantly reduced in the MI_{NF} hearts (**F**). In contrast, work per mass was reduced in all zones in the failing (MI_{CHF}) group compared with both sham and nonfailing (MI_{NF}). The estimated peak systolic stress was not significantly different between the groups in RZ and MZ, but elevated in AZ in the myocardial infarction (MI) animals compared with sham. (**G**). (Values reported are mean with SE.)

Disclosures

None.

References

1. Stefanon I, Valero-Muñoz M, Fernandes AA, Ribeiro RF Jr, Rodríguez C, Miana M, Martínez-González J, Spalenza JS, Lahera V, Vassallo PF, Cachofeiro V. Left and right ventricle late remodeling following myocardial infarction in rats. *PLoS One*. 2013;8:e64986. doi: 10.1371/journal.pone.0064986.
2. Espe EK, Aronsen JM, Eriksen GS, Zhang L, Smiseth OA, Edvardsen T, Sjaastad I, Eriksen M. Assessment of regional myocardial work in rats. *Circ Cardiovasc Imaging*. 2015;8:e002695. doi: 10.1161/CIRCIMAGING.114.002695.
3. Kramer CM, Lima JA, Reichek N, Ferrari VA, Llaneras MR, Palmon LC, Yeh IT, Tallant B, Axel L. Regional differences in function within noninfarcted myocardium during left ventricular remodeling. *Circulation*. 1993;88:1279–1288.
4. Cheng A, Nguyen TC, Malinowski M, Langer F, Liang D, Daughters GT, Ingels NB Jr, Miller DC. Passive ventricular constraint prevents transmural shear strain progression in left ventricle remodeling. *Circulation*. 2006;114(suppl 1):I79–I86. doi: 10.1161/CIRCULATIONAHA.105.001578.
5. Soleimanifard S, Abd-Elmoniem KZ, Sasano T, Agarwal HK, Abraham MR, Abraham TP, Prince JL. Three-dimensional regional strain analysis

in porcine myocardial infarction: a 3T magnetic resonance tagging study. *J Cardiovasc Magn Reson*. 2012;14:85. doi: 10.1186/1532-429X-14-85.
6. Kramer CM, Rogers WJ, Theobald TM, Power TP, Petruolo S, Reichek N. Remote noninfarcted region dysfunction soon after first anterior myocardial infarction. A magnetic resonance tagging study. *Circulation*. 1996;94:660–666.
7. Götte MJ, van Rossum AC, Twisk JWR, Kuijer JPA, Marcus JT, Visser CA. Quantification of regional contractile function after infarction: strain analysis superior to wall thickening analysis in discriminating infarct from remote myocardium. *J Am Coll Cardiol*. 2001;37:808–817.
8. Bogaert J, Bosmans H, Maes A, Suetens P, Marchal G, Rademakers FE. Remote myocardial dysfunction after acute anterior myocardial infarction: impact of left ventricular shape on regional function: a magnetic resonance myocardial tagging study. *J Am Coll Cardiol*. 2000;35:1525–1534.
9. Urheim S, Edvardsen T, Torp H, Angelsen B, Smiseth OA. Myocardial strain by Doppler echocardiography. Validation of a new method to quantify regional myocardial function. *Circulation*. 2000;102:1158–1164.
10. Russell K, Eriksen M, Aaberge L, Wilhelmsen N, Skulstad H, Remme EW, Haugaa KH, Opdahl A, Fjeld JG, Gjesdal O, Edvardsen T, Smiseth OA. A novel clinical method for quantification of regional left ventricular pressure-strain loop area: a non-invasive index of myocardial work. *Eur Heart J*. 2012;33:724–733. doi: 10.1093/eurheartj/ehs016.
11. Sjaastad I, Sejersted OM, Ilebekk A, Bjornerheim R. Echocardiographic criteria for detection of postinfarction congestive heart failure in rats. *J Appl Physiol*. 2000;89:1445–1454.
12. Dall'Armellina E, Jung BA, Lygate CA, Neubauer S, Markl M, Schneider JE. Improved method for quantification of regional cardiac function in mice using phase-contrast MRI. *Magn Reson Med*. 2012;67:541–551. doi: 10.1002/mrm.23022.
13. Espe EK, Aronsen JM, Skårdal K, Schneider JE, Zhang L, Sjaastad I. Novel insight into the detailed myocardial motion and deformation of the rodent heart using high-resolution phase contrast cardiovascular magnetic resonance. *J Cardiovasc Magn Reson*. 2013;15:82. doi: 10.1186/1532-429X-15-82.
14. National Center for the Replacement RaRoAiR. The 3Rs. 2017. National Center for the Replacement, Refinement and Reduction of Animals in Research. https://www.nc3rs.org.uk/. Accessed June 8, 2017.
15. Aronsen JM, Espe EKS, Skårdal K, Hasic A, Zhang L, Sjaastad I. Noninvasive stratification of postinfarction rats based on the degree of cardiac dysfunction using magnetic resonance imaging and echocardiography. *Am J Physiol Heart Circ Physiol*. 2017;312:H932–H942. doi: 10.1152/ajpheart.00668.2016.
16. Espe EK, Aronsen JM, Skrbic B, Skulberg VM, Schneider JE, Sejersted OM, Zhang L, Sjaastad I. Improved MR phase-contrast velocimetry using a novel nine-point balanced motion-encoding scheme with increased robustness to eddy current effects. *Magn Reson Med*. 2013;69:48–61. doi: 10.1002/mrm.24226.
17. Espe EK, Zhang L, Sjaastad I. Unwrapping eddy current compensation: improved compensation of eddy current induced baseline shifts in high-resolution phase-contrast MRI at 9.4 Tesla. *Magn Reson Med*. 2014;72:1096–1102. doi: 10.1002/mrm.25023.
18. Schneider JE, Wiesmann F, Lygate CA, Neubauer S. How to perform an accurate assessment of cardiac function in mice using high-resolution magnetic resonance imaging. *J Cardiovasc Magn Reson*. 2006;8:693–701. doi: 10.1080/10976640600723664.
19. Espe EK, Skardal K, Aronsen JM, Zhang L, Sjaastad I. A semiautomatic method for rapid segmentation of velocity-encoded myocardial magnetic resonance imaging data [published online ahead of print October 3, 2016]. *Magn Reson Med*. doi: 10.1002/mrm.26486. http://onlinelibrary.wiley.com/doi/10.1002/mrm.26486/abstract. Accessed August 9, 2017.
20. Pelc NJ, Drangova M, Pelc LR, Zhu Y, Noll DC, Bowman BS, Herfkens RJ. Tracking of cyclic motion with phase-contrast cine MR velocity data. *J Magn Reson Imaging*. 1995;5:339–345.
21. Zhu Y, Drangova M, Pelc NJ. Fourier tracking of myocardial motion using cine-PC data. *Magn Reson Med*. 1996;35:471–480.
22. Markl M, Schneider B, Hennig J. Fast phase contrast cardiac magnetic resonance imaging: improved assessment and analysis of left ventricular wall motion. *J Magn Reson Imaging*. 2002;15:642–653. doi: 10.1002/jmri.10114.
23. Russell K, Eriksen M, Aaberge L, Wilhelmsen N, Skulstad H, Gjesdal O, Edvardsen T, Smiseth OA. Assessment of wasted myocardial work: a novel method to quantify energy loss due to uncoordinated left ventricular contractions. *Am J Physiol Heart Circ Physiol*. 2013;305:H996–H1003. doi: 10.1152/ajpheart.00191.2013.
24. Frisk M, Ruud M, Espe EK, Aronsen JM, Røe ÅT, Zhang L, Norseng PA, Sejersted OM, Christensen GA, Sjaastad I, Louch WE. Elevated ventricular wall stress disrupts cardiomyocyte T-tubule structure and calcium homeostasis. *Cardiovasc Res*. 2016;112:443–451. doi: 10.1093/cvr/cvw111.
25. Nahrendorf M, Wiesmann F, Hiller KH, Han H, Hu K, Waller C, Ruff J, Haase A, Ertl G, Bauer WR. *In vivo* assessment of cardiac remodeling after myocardial infarction in rats by cine-magnetic resonance imaging. *J Cardiovasc Magn Reson*. 2000;2:171–180.
26. Hearse DJ. Species variation in the coronary collateral circulation during regional myocardial ischaemia: a critical determinant of the rate of evolution and extent of myocardial infarction. *Cardiovasc Res*. 2000;45:213–219.

CLINICAL PERSPECTIVE

Magnetic resonance imaging can accurately assess regional function in cardiac disease. However, there is an apparent discord in the literature on the function of the viable myocardium in the infarcted heart. The current study provides novel insight into regional myocardial function under different degrees of heart failure. In particular, we found that lack of increased function and higher level of negative work in the noninfarcted myocardium are related to global dysfunction and heart failure. Our study also underlines the added value of measuring myocardial work compared with strain alone.

Regional Dysfunction After Myocardial Infarction in Rats

Emil K.S. Espe, Jan Magnus Aronsen, Morten Eriksen, Ole M. Sejersted, Lili Zhang and Ivar Sjaastad

Circ Cardiovasc Imaging. 2017;10:
doi: 10.1161/CIRCIMAGING.116.005997
Circulation: Cardiovascular Imaging is published by the American Heart Association, 7272 Greenville Avenue, Dallas, TX 75231

Print ISSN: 1941-9651. Online ISSN: 1942-0080

SUPPLEMENTAL MATERIAL (Regional dysfunction after myocardial infarction in rats)

To evaluate the impact of the usage of group-specific standard LVP curves, we repeated the work calculations using a single normal curve.

One standard LVP curve was generated from the pressure measurements in the same 17 animals by normalizing to peak pressure and temporal matching to the valvular events.[2] We then redid all calculation of regional work and stress.

The results of the recalculation are shown in Figure S1. Compared to the results using the group-specific standard LVP curves (Figure 4), all group-wise differences in regional work were also present in the calculation with a single LVP normal curve.

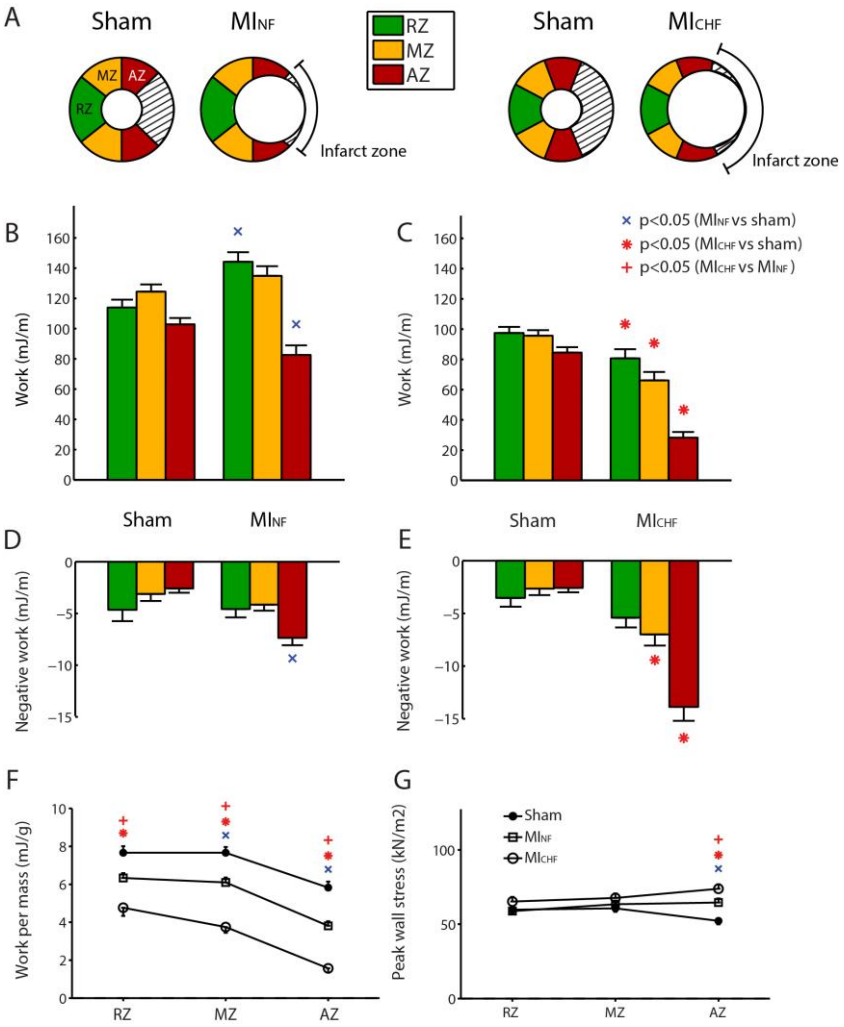
A
Sham
MI_NF
RZ
MZ
AZ
Sham
MI_CHF
Infarct zone
Infarct zone
B
Work (mJ/m)
C
× p<0.05 (MI_NF vs sham)
* p<0.05 (MI_CHF vs sham)
+ p<0.05 (MI_CHF vs MI_NF)
Work (mJ/m)
D
Sham
MI_NF
Negative work (mJ/m)
E
Sham
MI_CHF
Negative work (mJ/m)
F
Work per mass (mJ/g)
RZ
MZ
AZ
G
Sham
MI_NF
MI_CHF
Peak wall stress (kN/m2)
RZ
MZ
AZ

Figure S1